Clinical Cancer Research

Activated MET Is a Molecular Prognosticator and Potential Therapeutic Target for Malignant Peripheral Nerve Sheath Tumors

Keila E. Torres, Quan-Sheng Zhu, Katelynn Bill, et al.

Clin Cancer Res 2011;17:3943-3955. Published OnlineFirst May 3, 2011.

Published OnlineFirst May 3, 2011; DOI: 10.1158/1078-0432.CCR-11-0193

Human Cancer Biology

Clinical Cancer Research

Activated MET Is a Molecular Prognosticator and Potential Therapeutic Target for Malignant Peripheral Nerve Sheath Tumors

Keila E. Torres[1,4], Quan-Sheng Zhu[1,4], Katelynn Bill[2,4,6], Gonzalo Lopez[2,4,6], Markus P. Ghadimi[1,4], Xianbiao Xie[1,4], Eric D. Young[1,4], Juehui Liu[1,4], Theresa Nguyen[1,4], Svetlana Bolshakov[1,4], Roman Belousov[1,4], Suizhau Wang[1,4], Guy Lahat[1,4], Jun Liu[5], Belinda Hernandez[1,4], Alexander J. Lazar[3,4,6], and Dina Lev[2,4,6]

Abstract

Purpose: MET signaling has been suggested a potential role in malignant peripheral nerve sheath tumors (MPNST). Here, MET function and blockade were preclinically assessed.

Experimental Design: Expression levels of MET, its ligand hepatocyte growth factor (HGF), and phosphorylated MET (pMET) were examined in a clinically annotated MPNST tissue microarray (TMA) incorporating univariable and multivariable statistical analyses. Human MPNST cells were studied *in vitro* and *in vivo*; Western blot (WB) and ELISA were used to evaluate MET and HGF expression, activation, and downstream signaling. Cell culture assays tested the impact of HGF-induced MET activation and anti-MET–specific siRNA inhibition on cell proliferation, migration, and invasion; *in vivo* gel-foam assays were used to evaluate angiogenesis. Cells stably transduced with anti-MET short hairpin RNA (shRNA) constructs were tested for growth and metastasis in severe combined immunodeficient (SCID) mice. The effect of the tyrosine kinase inhibitor XL184 (Exelixis) targeting MET/VEGFR2 (vascular endothelial growth factor receptor 2) on local and metastatic MPNST growth was examined *in vivo*.

Results: All three markers were expressed in MPNST human samples; pMET expression was an independent prognosticator of poor patient outcome. Human MPNST cell lines expressed MET, HGF, and pMET. MET activation increased MPNST cell motility, invasion, angiogenesis, and induced matrix metalloproteinase-2 (MMP2) and VEGF expression; MET knockdown had inverse effects *in vitro* and markedly decreased local and metastatic growth *in vivo*. XL184 abrogated human MPNST xenograft growth and metastasis in SCID mice.

Conclusions: Informative prognosticators and novel therapies are crucially needed to improve MPNST management and outcomes. We show an important role for MET in MPNST, supporting continued investigation of novel anti-MET therapies in this clinical context. *Clin Cancer Res; 17(12); 3943–55. ©2011 AACR.*

Introduction

More effective therapies are crucially needed for the treatment of malignant peripheral nerve sheath tumors (MPNST). These highly aggressive and usually fatal sarcomas arise in proximity to peripheral nerves and develop sporadically (~50%) or within preexisting plexiform neurofibromas in patients with the neurofibromatosis type 1 (NF1; ~50%) genetic disorder. NF1 is a common autosomal dominant disorder with a prevalence of approximately 1:3,000 to 3,500 individuals worldwide (1–3). MPNSTs have limited sensitivity to chemotherapy or radiation; complete surgical resection remains the only potentially curative option for MPNST patients but is frequently not feasible because of local invasiveness and/or uncontrollable (primarily pulmonary) metastases (3). Accordingly, MPNSTs have a guarded prognosis; 20% to 50% 5-year patient survival rates have been reported and metastatic disease is ultimately fatal (1, 3–5).

The past decade has brought a remarkable interest in novel, molecularly targeted therapeutic regimens (6). The significant impact of interventions, such as Herceptin, a humanized anti-HER2 receptor antibody, and Gleevec, a KIT receptor small molecule inhibitor, on the outcome of patients with solid malignancies (breast cancer and GIST, respectively; refs. 7, 8) highlights both the relevance of tyrosine kinase receptors (TKR) as therapeutic targets and

Authors' Affiliations: Departments of [1]Surgical Oncology, [2]Cancer Biology, and [3]Pathology, [4]The Sarcoma Research Center, and [5]The Division of Quantitative Sciences, University of Texas MD Anderson Cancer Center; and [6]The Graduate School of Biomedical Sciences, Houston, Texas

Note: Supplementary Data for this article are available at Clinical Cancer Research Online (http://clincancerres.aacrjournals.org/).

Corresponding Author: Dina Lev, Department of Cancer Biology, MD Anderson Cancer Center, 1515 Holcombe Blvd, Unit 1104, Houston TX 77030. Phone: 713-792-1637; Fax: 713-563-1185; E-mail: dlev@mdanderson.org

doi: 10.1158/1078-0432.CCR-11-0193

Published OnlineFirst May 3, 2011; DOI: 10.1158/1078-0432.CCR-11-0193

Statement of Translational Relevance

More effective therapies are crucially needed for the treatment of malignant peripheral nerve sheath tumors (MPNST). These highly aggressive sarcomas are notorious for therapeutic resistance and are therefore frequently fatal. Previous studies have suggested a potential role for the HGF/MET autocrine loop in MPNST; data provided here confirm and expand these initial insights. Activated MET expression in human MPNST was found to be a prognosticator of shorter disease-specific survival (DSS), and MET targeting was shown to inhibit the migratory, invasive, and angiogenic phenotype of MPNST cells *in vitro* and *in vivo*. Most importantly, the orally available tyrosine kinase inhibitor XL184 which targets MET and VEGFR2, significantly abrogated local and metastatic growth of human MPNST xenografts. Taken together, these data offer new insights into MPNST molecular deregulations, identify a novel MPNST prognostic biomarker, and support further evaluation of anti-MET therapeutic strategies in the MPNST clinical setting.

the feasibility of developing compounds to block these highly accessible cell surface molecules (9). TKR overexpression and deregulated signaling has been identified in many malignancies, promoting tumor cell proliferation, aberrant cell-cycle regulation, and/or activation of signal transduction pathways mediating protumorigenic and prometastatic events. One such receptor is MET, also known as the hepatocyte growth factor receptor (HGFR). The MET ligand, hepatocyte growth factor (HGF; also called scatter factor), is a heparin-binding protein that is physiologically produced by a variety of mesenchymal cells. HGF induces pleiotropic biological activities, acting as a paracrine mitogen, motogen, and morphogen for epithelial cells that express the receptor (10). HGF stimulation induces the phosphorylation of several MET tyrosine residues (Y1003-Y1313-Y1230/1234/1235-Y1349-Y1365), which in turn activate multiple downstream pathways, including RAS/ERK (extracellular signal–regulated kinase), (phosphoinositide 3-kinase) PI3K/AKT, and SRC signaling (10, 11). Combined overexpression of MET and HGF has been reported in numerous carcinomas and sarcomas (12–14). MET signaling deregulations because of activating mutations, amplifications or via autocrine or paracrine growth factor loops have been described, suggesting a pivotal role for MET in tumorigenesis, disease progression, and metastasis (15–17); cancer-associated MET activation has been shown to trigger cell growth, survival, invasion, and angiogenesis (10, 18). These initial observations have prompted development of small molecule MET inhibitors. Such compounds have showed efficacy in preclinical studies *in vitro* and *in vivo*; several are currently being evaluated in human cancer clinical trials (19–21).

Several lines of evidence support a potential role for HGF/MET signaling in MPNST: (i) HGF has been found to be a mitogen for rat Schwann cells which normally express MET but not HGF (22); (ii) *MET* and *HGF* gene amplifications have been observed in human MPNST as per tumor specimen screening (23); (iii) HGF and MET proteins are concomitantly expressed in human MPNST samples (14); and (iv) anti-HGF antibody was found to inhibit MET activation in the ST88 MPNST cell line resulting in decreased invasive phenotype (24). Although limited by small numbers of testable specimens and cell lines, these initial insights strongly support further investigation of MET as a potential MPNST biomarker and therapeutic target.

Materials and Methods

Cell lines and reagents

Human MPNST cell lines ST88-14, STS26T, and MPNST724 were maintained and propagated as previously described (25); primary cultured normal human Schwann cells (NSC) served as controls. Additional cell line–related information including source and other cells used as controls is described in Supplementary Data. Authentication of cell lines was conducted utilizing Short Tandem Repeat DNA fingerprinting (STR; Supplementary Data and Table S1). The cytokines HGF and VEGF were purchased from R&D and the MET/VEGFR2 inhibitor, XL184 was kindly provided by Exelixis. Commercially available antibodies were used for immunoblot or immunohistochemical (IHC) detection of: MET, phosphorylated (pMET; Tyr1234/Tyr1235 and Tyr1349), AKT, pAKT (Ser473), ERK, pERK, RET, VEGF, VEGFR2, pVEGFR2, AXL, KIT (Cell Signaling), HGF, matrix metalloproteinase-2 (MMP2; R&D Systems), CD31, (Pharmingen), goat anti-rat HRP (Jackson ImmunoResearch Laboratories, Inc.), DeadEnd Fluorometric TUNEL System (Promega), Ki67 (Thermo/Lab Vision), and β-actin (Santa Cruz Biotechnology).

Clinically annotated tissue microarray

A recently established tissue microarray (TMA)-containing tissues retrieved from 96 MPNST surgical specimens (NF1 associated = 55, sporadic = 41) was used (3). This TMA also includes 4 evaluable samples of normal nerves (brachial, sciatic, supraclavicular, and cervical) which were evaluated as controls. A comprehensive clinical database containing patient, tumor, treatment, and follow-up information linked to TMA has previously constructed and has been updated to enable current analysis.

Immunohistochemistry

TMA immunostaining and xenograft derived specimens immunohistochemistry and terminal deoxynucleotidyl transferase-mediated dUTP nick end labeling (TUNEL) staining were conducted as we have previously described (3, 26). For TMA analysis, each biomarker was scored by 2 independent observers (G.L. and A.L.) after excluding spots with insufficient tumor tissue or those that detached from the slide as sometimes occurs on TMAs as the result of the IHC process. Intensity was graded as none (= 0), weak/low (= 1), or moderate-to-strong/high (= 2 to 3), and the

Published OnlineFirst May 3, 2011; DOI: 10.1158/1078-0432.CCR-11-0193

percentage of positive tumor cells was estimated. Similarly, staining distribution (% positive-stained tumor cells) and intensity (0 = no staining, 1 = low, 2 = high) as well as CD31 counts (in 10× HPF) of xenograft tissues were evaluated and scored by 2 independent reviewers (K.T. and E.Y.).

Cellular assays

More detailed information is available as Supplementary Data. In brief; MTS and clonogenicity assays were conducted as previously described (26). Western blot (WB) analyses were carried out by standard methods (26). Enzyme-linked immunosorbent assay (ELISA) HGF and VEGF levels were measured in MPNST cell conditioned media (CM) using ELISA. The assays were constructed and preformed following manufacturer's instructions (R&D). Migration and invasion assays were conducted using modified Boyden chambers as previously described (27). Quantitative real-time PCR (qRT-PCR) for MMP2 was conducted as previously described (28). MET gene sequencing procedure and primers, as well as siRNA and short hairpin RNA (shRNA) transfection and transduction procedures are detailed in Supplementary Data.

In vivo animal experiments

All animal procedures/care was approved by UTMDACC Institutional Animal Care and Usage Committee. Animals received humane care as per the Animal Welfare Act and the NIH "Guide for the Care and Use of Laboratory Animals". *In vivo* Gelfoam angiogenesis assay and animal models were utilized as previously described (29, 30). Information regarding animal models and therapeutic schemas are provided in Supplementary Data.

Statistics

A Spearman's test was used to test correlation between HGF and pMET expression in human MPNST specimens and cell lines. To evaluate the correlation of TMA biomarker expression and patient disease-specific survival (DSS; defined as the time interval from the date of presentation to MD Anderson to the date when the patient dies of MPNST or to the last follow-up date, whichever occurred first), each independent variable was first examined separately in a univariable Cox proportional hazards model. All univariable Cox models were fitted with all possible data points. For all outcomes, only the independent variables that had P values of 0.10 or less in the univariable Cox model analyses were examined in multivariable Cox models; $P \leq 0.05$ was set as the cutoff. Cell culture–based assays were repeated at least twice; the means and SD were calculated for each assay. Cell lines were examined separately. For outcomes that were measured at a single time point, 2 sample t tests were used to assess the differences. A mixed effect model was used to assess differences in xenograft growth over time between treatment and control groups. Differences in xenograft size and weight (tumor/metastases) between treatment and control groups at study termination were assessed using a 2-tailed Student's t test. Significance was set at $P \leq 0.05$. All computations were conducted in SAS 9.1 (SAS Institute) and Splus 7.0 (Insightful Corporation).

Results

HGF and MET are highly expressed in human MPNST samples: pMET expression levels correlate with shorter MPNST-specific survival

We have recently reported the overexpression of several TKRs, including MET, in MPNST utilizing our TMA (31). Here, we aimed to further examine the expression of HGF and activated MET (pMET; Fig. 1A); all MPNST samples on the TMA were evaluated when available. All MPNSTs expressed MET: low levels were observed in 9% ($n = 9$) and moderate-to-high in 91% ($n = 87$), an average of 92% (±8%) of tumor cells per sample exhibited positive MET staining. Similarly, all (100%) of MPNSTs expressed HGF: low levels were found in 43% ($n = 39$) and intermediate to high expression levels were noticed in 57% ($n = 51$) of cases, an average of 60% (±24%) of tumor cells per sample exhibited positive HGF staining. pMET expression was found in 51% ($n = 45$) of MPNSTs, no pMET expression could be found in the remainder of samples; pMET staining (in samples that expressed pMET) was exhibited on average in approximately 30% (±20%) of tumor cells. A strong correlation between pMET and HGF expression was identified (correlation coefficient: 0.45, $P = 0.003$; Spearman's test). It is of note, however, that not all specimens expressing both MET and HGF exhibited activated MET. It is known that HGF is secreted as an inactive zymogen that is further activated by protease cleavage (32). To that end HGF/MET autocrine loop can only be functional when these HGF activators are also present possibly explaining the above described scenario. This association has previously been reported in MPNST (24). Interestingly, metastatic MPNST lesions ($n = 15$) expressed higher pMET intensity (average 1 ± 0.67 vs. 0.44 ± 0.58) and distribution (22% ± 24% vs. 11% ± 17%) as compared with localized (primary and recurrent) lesions ($n = 55$). No difference in expression of any marker could be showed when comparing NF1-associated with sporadic MPNST. Of note, MET expression was found in all 4 normal nerve sheath samples (low intensity = 2, moderate intensity = 2) but only minimal HGF (none to very weak) was seen and no pMET was observed in these samples (Fig. 1A).

Next, we evaluated whether marker expression intensity and distribution correlated with DSS of patients with localized MPNST ($n = 55$). A univariable analysis failed to identify HGF and MET expression levels as predictive of shorter patient survival (Supplementary Table S2). In contrast, and of potential major clinical importance, high pMET expression levels and increased percentage of positive cells were found to be prognosticators of unfavorable DSS ($P = 0.012$ and 0.0004, respectively). pMET expression was also found to be an independent prognosticator ($P = 0.014$) based on a multivariable analysis which included factors previously shown to have independent prognostic value [i.e., p53 expression, tumor size ≥ 10 cm, and loss of

Published OnlineFirst May 3, 2011; DOI: 10.1158/1078-0432.CCR-11-0193

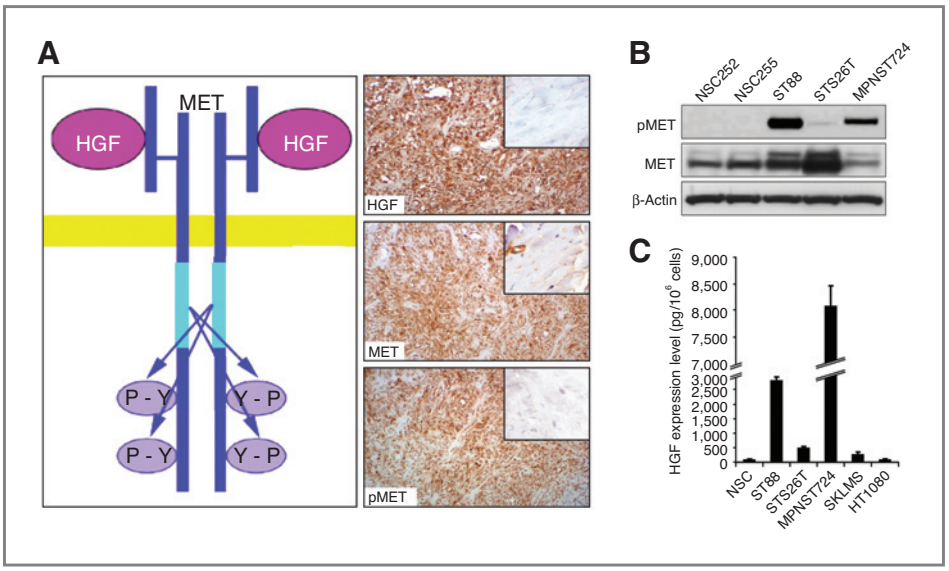

Figure 1. MET is highly expressed and activated in human MPNST. A, representative photographs of MPNST TMA HGF, MET, and pMET (Tyr1234/Tyr1235) immunostaining (insets depict corresponding IHC staining in normal nerve sheath; original images were captured at 200× magnification). B, WB analysis demonstrating the expression of MET and pMET (Tyr1234/Tyr1235) in human MPNST cell lines (NF1-associated: ST88, T265 and sporadic: 26T, MPNST724) and NSC (NSC252 and NSC255). C, HGF secretion by MPNST cells was measured by ELISA. NSC and the human soft tissue sarcoma cells SKLMS1 (leiomyosarcoma) and HT1080 (fibrosarcoma) were used as controls. (Graphs represent the average of 3 repeated experiments ± SD).

S100 protein expression (3)]. Interestingly, tumor size and decreased S100 expression lost their independent status with the inclusion of pMET in this analysis. These findings strongly support the potential clinical applicability of studies focusing on the MET pathway in the context of MPNST.

HGF, MET, and constitutively activated MET are highly expressed in human MPNST cell lines

Next, we evaluated whether human MPNST cell lines express MET and thus can be used to further evaluate the potential function of this receptor in MPNST (Fig. 1B). WB analysis showed increased MET expression in ST88 and STS26T MPNST cell lines compared with NSC; MPNST724 cells did express MET, albeit at comparatively lower levels. Most importantly, constitutive phosphorylation of MET to varying degrees was found in all MPNST cells but not in NSC. No direct correlation between total MET and pMET expression could be found; that is, STS26T cells, (highly MET expressive), exhibited the lowest pMET levels, whereas MPNST724 exhibited lower MET levels yet expressed a relatively high level of pMET. MET activating mutations have been described for various human tumors (15, 17, 33, 34). To address whether the observed activation of MET in MPNST cells could be secondary to such mutations, we sequenced the *MET* gene: no mutations in the IPT repeat (exon 10), the juxtamembrane (exons 13–15), and the kinase (exons 16–19) could be found.

To further determine whether MET activation is secondary to an HGF autocrine loop, we evaluated the expression of cell-secreted HGF (Fig. 1C): MPNST cells were found to express high levels of HGF as compared with either NSC (exhibiting no HGF expression) or 2 other soft tissue sarcoma cell lines serving as controls. These findings taken together suggest that HGF and MET may possibly form an autocrine signaling loop in human MPNST cells.

MET activation enhances MPNST migratory, invasive, and angiogenic phenotypes

Next, we evaluated whether HGF can induce further MET phosphorylation in MPNST cells and also determined the functional consequences of MET activation. Figure 2A shows that HGF stimulation (50 ng/mL for 20 minutes) results in increased pMET (Tyr1234/1235) expression in serum-starved MPNST cells; in turn leading to downstream activation of the PI3 kinase and the mitogen-activated protein kinase (MAPK) pathways. Of note, pMET levels were found to be generally lower when MPNST cells were cultured in serum-free media as compared with serum-containing conditions; no decrease in HGF levels was found under these culture conditions (data not shown), suggesting that other mechanisms are possibly responsible for this observed pMET decrease. No significant effect on MPNST growth was detected secondary to HGF stimulation as evaluated by MTS (24 and 48 hours) and clonogenicity (10 days) assays (Supplementary Fig. S1A and B). However, a significant increase in cell migration and invasion, 2 cellular functions critical for local aggressiveness and distant metastasis was noticed using modified Boyden chamber assays (12 hours; Fig. 2B). NSC do express MET, but unlike MPNST cells these normal cells do not exhibit constitutive MET phosphorylation and do not secret high levels of the ligand HGF (Fig. 1B and C). On HGF stimulation (at same doses as for MPNST cells) increase in MET

Published OnlineFirst May 3, 2011; DOI: 10.1158/1078-0432.CCR-11-0193

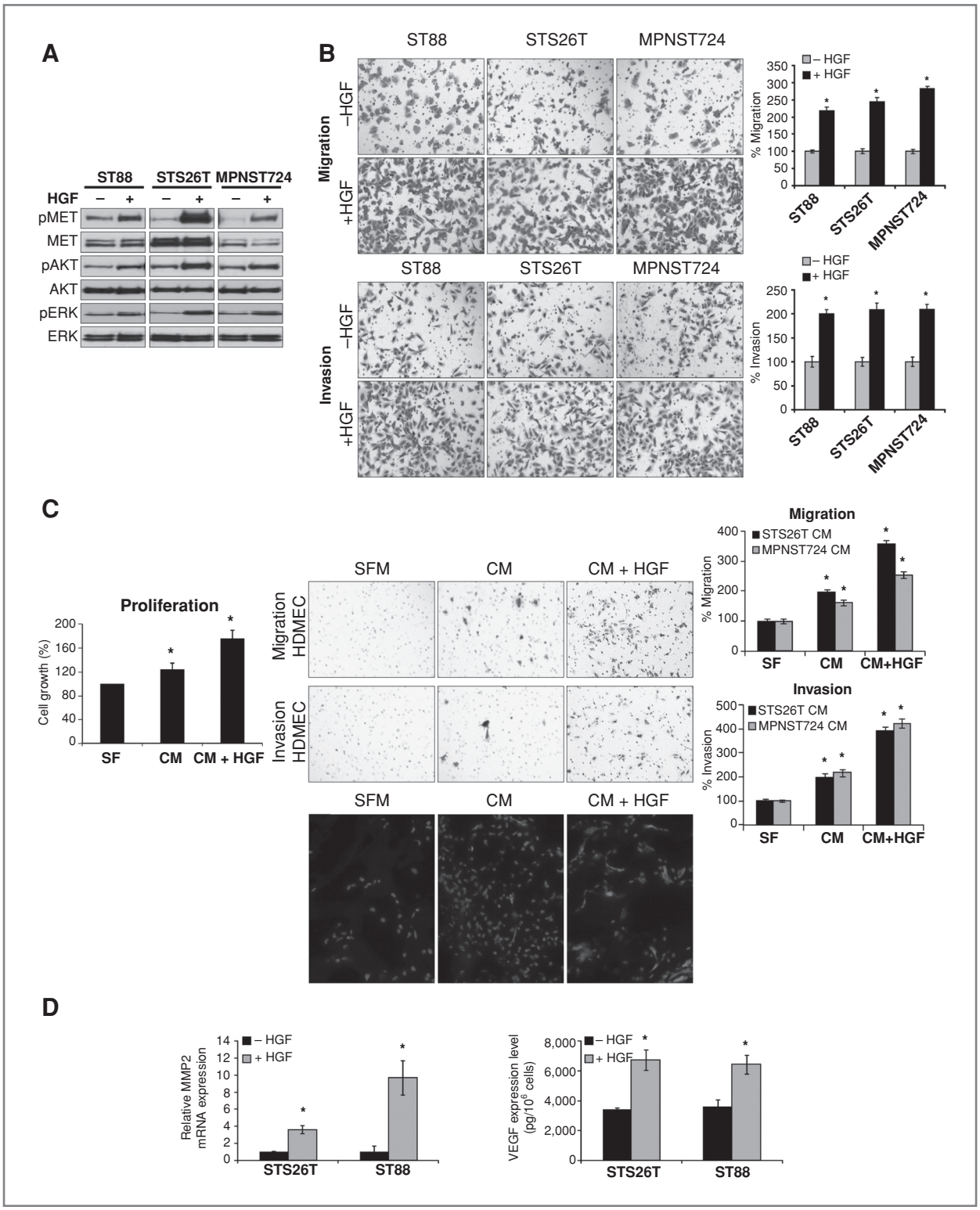

Figure 2. MET activation enhances MPNST cell migratory, invasive, and angiogenic phenotype. A, WB depicting enhanced MET phosphorylation and downstream signaling (through AKT and ERK) in response to HGF. Cells were grown in serum-free media overnight prior to HGF stimulation. B, enhanced MPNST migration and invasion in response to HGF stimulation was identified using modified Boyden chamber assays; C, MPNST cell collected CM (i.e. MPNST cells were stimulated with HGF (or no HGF) for 24 hours, after careful washing, fresh serum-free media was added and collected after 24 hours) enhanced the growth of HDMECs (MTS assays, STS26T cells are shown; upper left graph). Similarly, MPNST cell collected CM, especially from cells prestimulated with HGF increased HDMEC migration and invasion (right panel). Lastly, an *in vivo* gel foam assay showed that HGF-stimulated MPNST cell CM significantly enhances angiogenesis (evaluated via CD31 immunofluorescence), D, HGF stimulation enhances MMP2 mRNA expression (qRT-PCR) and VEGF protein expression (ELISA) in MPNST cells. [Graphs represent the average of at least 2 repeated experiments ± SD; *, denotes statistically significant effects ($P < 0.05$)]

Published OnlineFirst May 3, 2011; DOI: 10.1158/1078-0432.CCR-11-0193

phosphorylation was observed (Supplementary Fig. S2A); no significant effect on proliferation was seen (Supplementary Fig. S2B) but increase in migration and invasion was noted (Supplementary Fig. S2C). These data show that HGF is a NSC motogen, and it is possible that, as commonly occurs in cancer, MPNST cells "hijack" this physiologic function and by simultaneously expressing both the receptor and the ligand acquire an aggressive phenotype.

MPNST growth and dissemination, analogous to other solid malignancies, depends on cross-talk between tumor and tumor-associated normal cells. MPNSTs are generally highly vascular and angiogenic, facilitating metastatic potential. Consequently, we sought to evaluate whether MET activation enhanced the pro-angiogenic capacity of MPNST cells. Toward that end, serum starved MPNST cells were treated with HGF for 24 hours or with no HGF (control). Fresh media was added to the cells after repeated washings (i.e., no exogenous HGF present) and was collected after 24 hours. Incubation of human dermal microvessel endothelial cells (HDMEC) with CM collected from cells pretreated with HGF enhanced the proliferation and, most significantly, the migration and invasion of these endothelial cells, as compared with incubation with CM collected from MPNST cells not treated with HGF or HDMECs cultured in serum-free media alone (Fig. 2C). Moreover, an increased number of CD31 positive blood vessels were found in gel foams resuspended in HGF-pretreated MPNST CM, an assay of *in vivo* angiogenesis (Fig. 2C).

Our data suggest that HGF-induced MET activation enhances the migratory, invasive, and angiogenic phenotype of MPNST cells. Of potential importance, we found that MET activation induces MMP2 mRNA expression (qRT-PCR) and VEGF protein secretion (ELISA) by MPNST cells (Fig. 2D). These factors are known to contribute to migration, invasion, and/or angiogenesis and their induction may, at least in part, underlie the functional effects noted above.

MET knockdown induces anti-MPNST effects *in vitro* and *in vivo*

Next, we knocked down MET in MPNST cells using anti-MET–specific siRNA (20 nmol/L pool); nontargeting siRNA (a pool of 4 nontargeting constructs) was used as control. A significant decrease (~40% and ~75% in STS26T and MPNST724, respectively) in total MET protein expression was achieved after this knockdown (Fig. 3A; densitometry data depicted in Fig S3). Most importantly, MET knockdown blocked ligand-induced activation of MET and resultant downstream signaling. MET knockdown did not affect cell growth and proliferation (data not shown) but significantly inhibited constitutive and HGF-induced cell migration and invasion (Fig. 3B). These data confirm the observations described above and further support an important role for MET in the MPNST migratory and invasive phenotype.

Most importantly, we sought to evaluate if MET functional effects were operative *in vivo*. To achieve stable MET knockdown in MPNST cells, we first screened several shMET constructs to determine their knockdown efficiency (Supplementary Fig. S1C). Constructs 1 and 4 were found to significantly inhibit MET expression and were subsequently used for stable lentiviral shRNAs transduction; a nontargeting shRNA was used as control. Stable MET knockdown blocked HGF-induced MET phosphorylation and downstream signaling (Fig. 3C). As with transient MET knockdown, no significant effect on tumor cell growth was seen (Supplementary Fig. S1D); however, a marked reduction in constitutive and HGF-regulated migration and invasion was found (Fig. 3D). MET knockdown blocked HGF-mediated induction of MMP2 and VEGF expression (Fig. 3D).

Next, the growth of MET shRNA (constructs 1 and 4) STS26T-transduced cells was evaluated *in vivo;* nontargeting shRNA-transduced cells were used as controls. As depicted in Figure 4A, MET knockdown xenografts showed slower growth ($P < 0.001$) and a significantly decreased volume at study termination as compared with control tumors (0.10 ± 0.01 g and 0.10 ± 0.01 g vs. 0.52 ± 0.2 g; $P < 0.001$). IHC studies confirmed decreased MET expression in tumors originating from METshRNA-transduced cells (Fig. 4B). MET-knocked down tumors exhibited decreased microvessel density (measured by CD31 staining), increased apoptosis (measured via TUNEL), decreased proliferation (measured by Ki67), and decreased MMP2 and VEGF expression. As no effect on proliferation of MPNST cells was noted *in vitro* after MET blockade, it is possible that the marked differences observed in xenografts growth are secondary to the antiangiogenic effects elicited by of MET knockdown.

Finally, we evaluated the impact of MET knockdown on MPNST metastasis growth utilizing an experimental lung metastasis approach. All 5 NTshRNA intravenously injected mice exhibited extensive lung metastases; no macroscopic metastases were found in 3 of the METshRNA1 mice and only isolated metastases (≤ 3) were found in the additional 2 mice. A similar metastatic pattern was seen in METshRNA4-injected mice. Average lung weight of NTshRNA-injected mice was 0.88 ± 0.36 g compared with 0.34 ± 0.21 g and 0.37 ± 0.17 g in MET1shRNA and MET4shRNA intravenously injected mice, respectively (Fig. 4C). Taken together, these data suggest that MET contributes to local and metastatic MPNST growth and tumor-associated angiogenesis.

The multi-kinase MET/VEGFR2 inhibitor, XL184, exerts marked anti-MPNST effects *in vitro* and *in vivo*

Seeking to further show a potential role for MET in MPNST, we evaluated the impact of the small molecule multi-tyrosine kinase inhibitor XL184 (targeting MET and VEGFR2; Exelixis) on MPNST growth. Marked inhibition of constitutive and inducible MET phosphorylation and its resultant downstream signaling was observed in all MPNST cells tested after 4-hour incubation with XL184 at doses as low as 0.1 to 0.5μmol/L (Fig. 5A and S4A). No VEGFR2 expression could be identified in MPNST cells

Published OnlineFirst May 3, 2011; DOI: 10.1158/1078-0432.CCR-11-0193

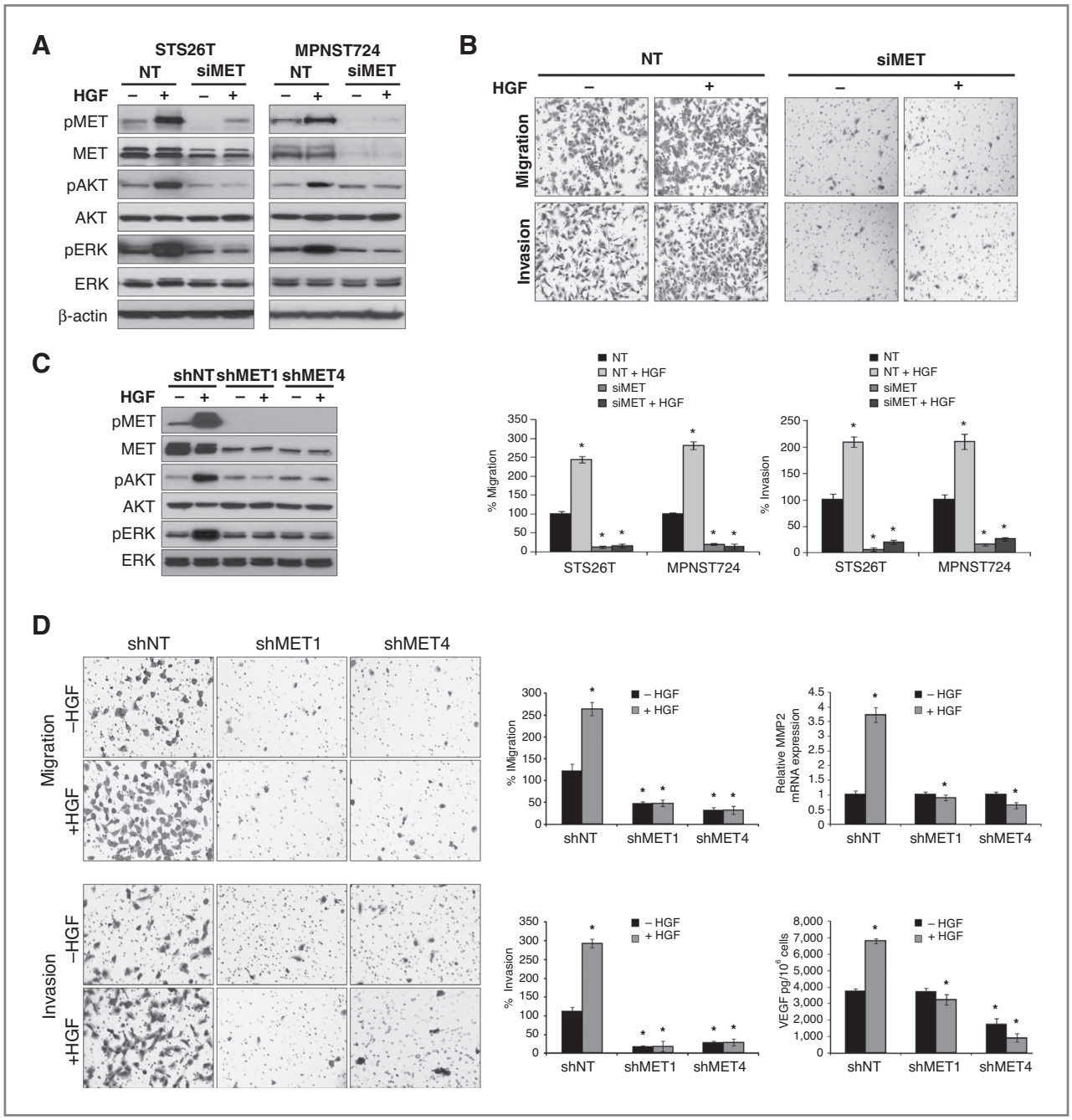

Figure 3. MET knockdown inhibits MPNST cell migration and invasion. A, anti-MET siRNA (siMET; 20 nmol/L pool) knockdown (KD) resulted in a significant decrease in MET expression and blocked HGF-induced MET activation and downstream signaling in MPNST cells. Nontargeting siRNA construct transfection was used as control (relative protein expression levels per densitometry are depicted in Supplementary Fig. S3); B, MET KD inhibited both constitutive and HGF-induced MPNST cell migration and invasion. C, STS26T (shown) and MPNST724 cells were stably transduced with 2 different shMET (shMET1 and shMET4) constructs that were found to markedly inhibit MET expression; NT shRNA construct was used as control (shNT). KD inhibited MET phosphorylation and downstream signaling. D, as with siRNA, stable shMET significantly blocked MPNST cell migration and invasion (results of STS26T cells are shown). MET KD blocked HGF-induced MMP2 mRNA (qRT-PCR) and VEGF protein (ELISA) expression. [*, denotes statistically significant effects ($P<0.05$)]

(Supplementary Fig. S4B), thus inhibitory activity of XL184 on VEGFR2 is possibly more relevant in an *in vivo* setting, blocking the activity of this receptor on tumor-associated endothelial cells. XL184 does induce marked inhibition of MET and VEGFR2 phosphorylation in cytokine-stimulated human umbilical vein endothelial cells (HUVECs ; Fig. 5A).

Only minimal impact on growth was seen with low XL184 doses (0.1μmol/L for 48 hours) although MET

Published OnlineFirst May 3, 2011; DOI: 10.1158/1078-0432.CCR-11-0193

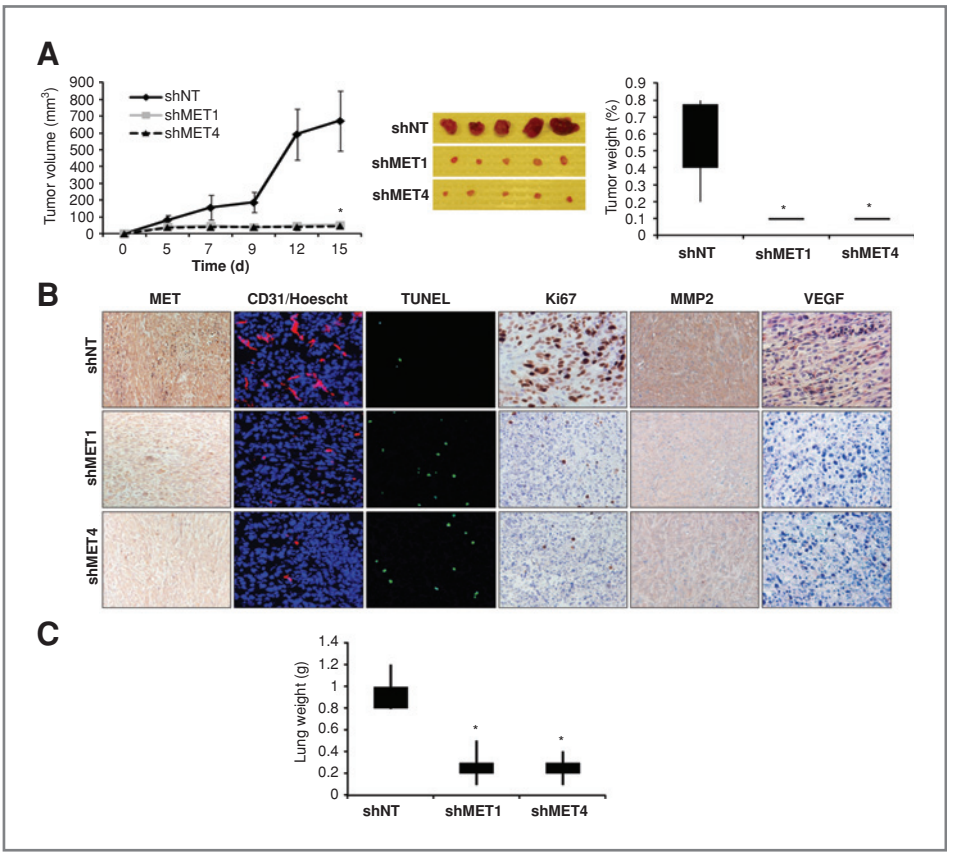

Figure 4. MET knockdown inhibits MPNST local and metastatic growth *in vivo*. A, ShMET-transduced STS26T cells were evaluated for local growth in SCID mice. MET KD xenografts exhibited slower growth (left graph; $P < 0.001$), decreased size at study termination (middle panel; $P < 0.001$), and a significantly decreased weight (right graph; $P < 0.001$) at study termination as compared with control shNT xenografts. B. IHC staining confirmed decreased MET expression in tumors originating from METshRNA-transduced cells. MET KD tumors exhibited decreased microvessel density (measured by CD31 staining), increased apoptosis (measured via TUNEL), decreased proliferation (measured by Ki67, control magnification is 200×, shMET1 and shMET4 magnification is 40×, reflecting a larger field of cells), and decreased MMP2 and VEGF expression. C, average lung weight of NT shRNA tail vein injected mice was markedly higher than that of MET KD cells injected mice reflecting a significantly decreased metastatic load. [*, denotes statistically significant effects ($P < 0.05$)]

inhibition at this dose was evident (Fig. 5B). However, increased XL184 doses did elicit a significant MPNST cell growth inhibition; higher XL184 doses were needed to inhibit NSC growth (Supplementary Fig. S2B). Although, the MET and VEGFR2 might be the most MPNST-relevant targets in this experimental setting, additional biologically relevant effects might be exerted through inhibition of other cancer-specific XL184 targets such as AXL, RET, and KIT (35). MPNST cells were found to express varying levels of these receptors (Supplementary Fig. S4B) possibly explaining the observed decrease in cell growth with increasing XL184 doses. Next, we evaluated whether XL184 (0.5 μmol/L) could inhibit MPNST cell migration and invasion. Cells were pretreated with XL184 for 4 hours and plated without the inhibitor in modified Boyden chambers. As depicted in Fig. 5C, XL184 treatment blocked HGF-induced MPNST motility and invasion (a similar effect of found on NSC [Supplementary Fig. S2C]). Lastly, we evaluated the effect of XL184 on MPNST cytokine rich CM induced angiogenesis. An *in vivo* gel foam assay was conducted as per above and mice were treated with XL184 (30 mg/kg) or vehicle for 10 days. A significant decrease in microvessel density was observed (Fig. 5D). Taken together, these findings possibly reflect the potential anti-tumor and, most importantly, anti-metastatic effects of XL184 in MPNST.

To determine whether the *in vitro* observations could be recapitulated *in vivo*, we conducted a series of therapeutic experiments using xenograft severe combined immunodeficient (SCID) mice models. A XL184 dose of 30 mg/kg/day given orally was selected based on the previous observation that this therapeutic dose results in greater than 90% tumoral pMET inhibition *in vivo* (as compared with ~50% when a dose of 10 mg/kg is administered; (36). The difference in XL184 potency between cells in culture and tissue in mice (PK experiments show C_{max} values of 13.7 μmol/L in nude mice plasma at the dose above; personal communication) is protein binding, which is greater than 99% in plasma. To that end, the dose selected for mice experiments is likely biologically comparable with that used in cell culture experiments.

First, we investigated the effect of XL184 on STS26T growth (Fig. 6A); therapy was initiated after tumor establishment (~5 mm in larger dimension). This treatment regimen was highly tolerated; no significant weight loss was observed. XL184-treated tumors exhibited a significantly slower growth ($P < 0.001$). Moreover, treatment with XL184 significantly reduced tumor size ($P < 0.001$) and weight compared with control ($P = 0.008$); average tumor weights at study termination were 0.84 g (SD ± 0.5) and 0.11 g (SD ± 0.06) in control and XL184 groups, respectively. To even more closely mimic a clinically relevant

Published OnlineFirst May 3, 2011; DOI: 10.1158/1078-0432.CCR-11-0193

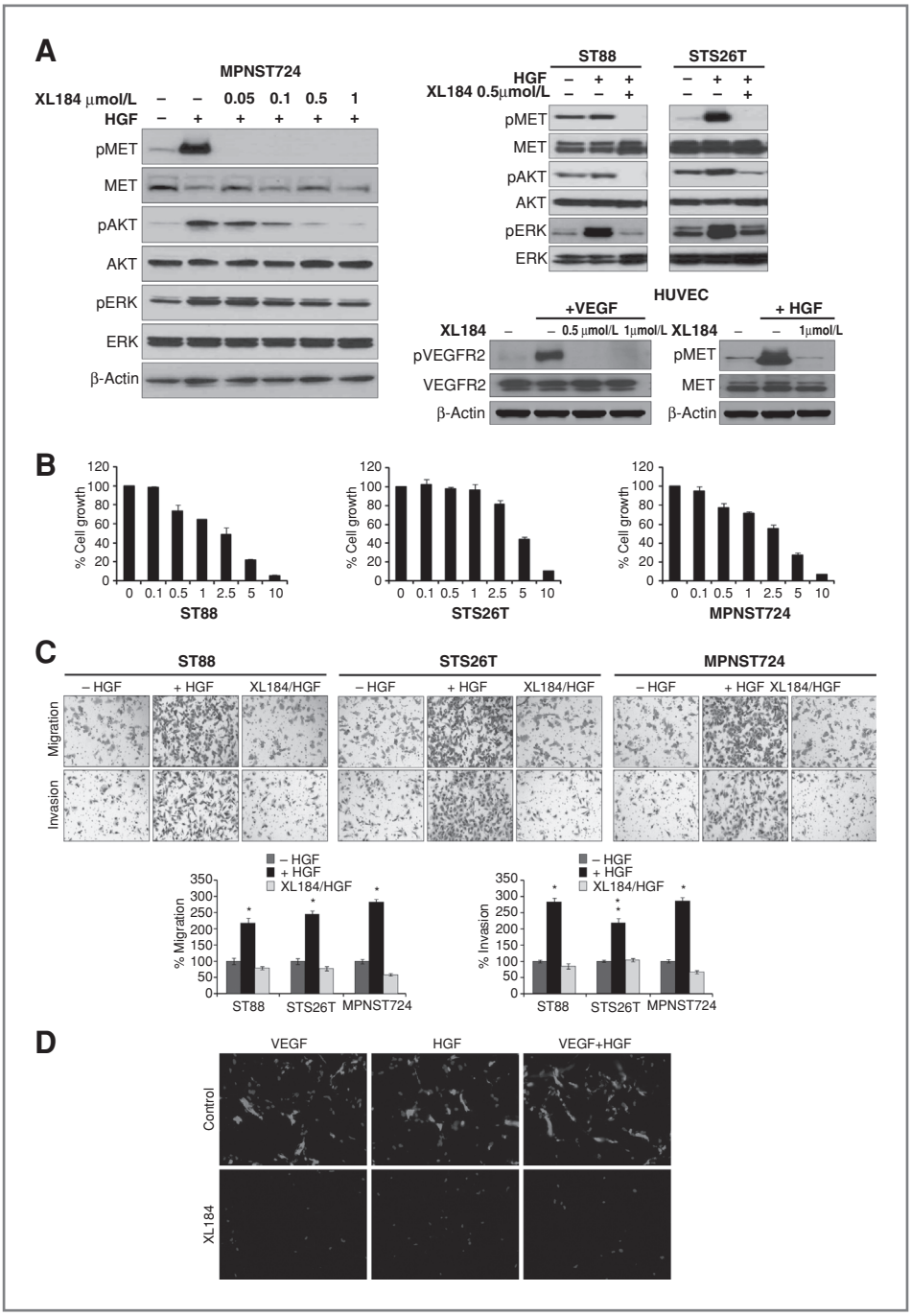

Figure 5. The multi-tyrosine kinase inhibitor, XL184, targeting MET and VEGFR2 abrogates MPNST migration, invasion, and angiogenesis. A, marked inhibition of constitutive and inducible MET phosphorylation and its resultant downstream signaling was observed after 4 hours incubation with XL184 at doses as low as 0.05 to 0.5 μmol/L in MPNST cell lines. XL184 induced marked inhibition of VEGFR2 and MET phosphorylation in cytokine stimulated HUVECs. B, no significant effect on MPNST cell growth was seen with low XL184 doses (0.1 μmol/L for 48 hours) although MET inhibition at this dose was identified as per above. However, increased XL184 doses did elicit marked MPNST cell growth inhibition. C, relatively low XL184 doses (0.5 μmol/L for 4 hours) inhibited HGF-induced MPNST cell migration and invasion. D, An *in vivo* gel-foam assay showed a dramatic decrease in cytokine-induced angiogenesis [microvessel density was determined based on CD31 immunofloresence (red)] in response to XL184 treatment (30 mg/kg/day for 10 days). [*, denotes statistically significant effects ($P < 0.05$)]

scenario, the above experiment was repeated but treatment was initiated later when tumors reached a larger size (~7–9 mm in largest dimension; Fig. 6A). XL184 significantly halted tumor growth ($P < 0.001$) and reduced tumor weight ($P = 0.002$) compared with control; average tumor weights at study termination were 0.98 g (SD ± 0.3) and 0.27 g (SD ± 0.16) in control and XL184 groups, respectively.

Finally, to confirm that XL184 anti-MPNST effects were not STS26T xenograft specific, we also utilized the MPNST724 model to assess therapeutic effects, demonstrating significant antitumor effects of XL184 treatment in this model as well ($P < 0.001$; Fig. 6B). At the time point mandating control mouse euthanasia, average volumes of vehicle-treated tumors were 1,609 μL ± 493 as compared with 17 μL ± 12 of the XL184-treated tumors ($P < 0.001$). XL184 treatment was continued for an additional 12 days with no evidence of tumor regrowth. Comparing the effects of XL184 on STS26T and MPNST724 xenografts, a more

Published OnlineFirst May 3, 2011; DOI: 10.1158/1078-0432.CCR-11-0193

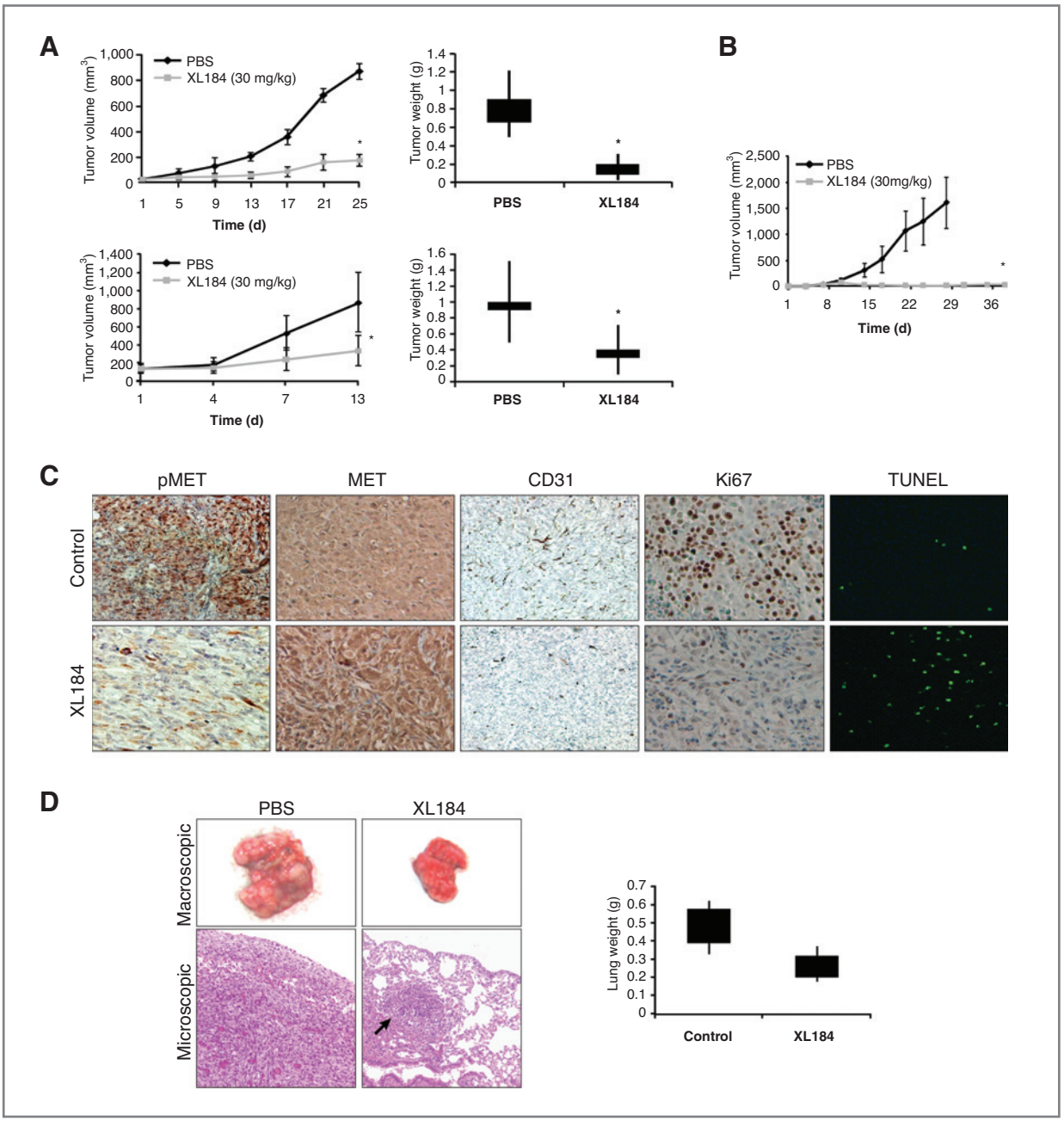

Figure 6. XL184 abrogates local and metastatic MPNST growth *in vivo*. A, SCID mice bearing STS26T xenografts (~5mm in average larger dimension) were treated with XL184 ($n = 8$ mice; 30 mg/kg) or vehicle only ($n = 7$ mice). XL184 markedly abrogated tumor growth ($P < 0.001$; left top graph). Moreover, treatment with XL184 significantly reduced tumor weight compared with control ($P = 0.008$; right top graph). Experiment was repeated but treatment was initiated later when STS26T xenografts reached a larger size (~7 to 9mm in largest dimension). XL184 significantly halted tumor growth ($n = 9$ mice; bottom left graph) as compared with control ($n = 9$ mice; $P < 0.001$) and reduced tumor weight ($P = 0.002$; bottom right graph); B. similarly, a significant anti-tumor effect was found with XL184 treatment of MPNST724 xenografts ($n = 10$ mice in each arm XL184 vs control). XL184 was continued for 12 days after control mice euthanasia with no evidence of tumor regrowth. C, based on IHC analysis, XL184 treatment inhibited MET phosphorylation without demonstrable impact on total MET expression levels. Furthermore, a pronounced decrease in number of tumor-associated blood vessels (showed by CD31 positivity), a marked decrease in MPNST cell proliferation (Ki67 staining), and a demonstrable increase in tumor cell apoptosis (TUNEL positivity) was observed in XL184-treated tumors. D, STS26T lung metastases bearing mice were treated with XL184 ($n = 8$ mice). At study termination, lungs of control mice ($n = 8$ mice) were almost completely replaced by tumor (left panel) whereas only isolated lesions were found in 2 mice of the XL184-treated group. Macroscopic findings were also confirmed on H+E staining, demonstrating large lung tumor deposits in control and only small or no microscopic lesions in XL184 groups. A significant difference in average lung weight was found between control and XL184-treated mice ($P = 0.002$; right panel). [*, denotes statistically significant effects ($P < 0.05$)].

Published OnlineFirst May 3, 2011; DOI: 10.1158/1078-0432.CCR-11-0193

pronounced antitumor effect was noted in the latter where tumor regression was observed; in STS26T tumors, XL184 induced a marked and statistically significant decrease in growth rate but not tumor abrogation. Future studies to identify additional therapies that can be used in combination with XL184 to further enhance cytotoxicity might be warranted.

Tumor sections containing viable cells from each experimental arm were selected for IHC studies. To first confirm that XL184 blocked MET phosphorylation *in vivo*, immunostaining for pMET was carried out. Figure 6C shows the marked inhibition of MET activation in the XL184-treated group without comparable impact on total MET expression levels. Furthermore, a pronounced decrease in number of tumor-associated blood vessels was observed (showed by CD31 positivity), confirming the antiangiogenic, antivascular effects of XL184. XL184 treatment resulted in marked decrease in MPNST cell proliferation, and a demonstrable increase in tumor cell apoptosis.

Finally, to evaluate whether XL184 resulted in pulmonary metastastic outgrowth inhibition, we utilized the STS26T experimental MPNST lung metastasis model. Treatment was initiated a week after tail vein injection (lung metastases can usually be found at this time), mice were followed and then sacrificed after 3 weeks. Lungs of control mice ($n = 8$) were almost completely replaced by tumor (Fig. 6D). In contrast, isolated lung metastases could be found in only 2 of the XL184 and no macroscopic disease was visualized in 6 additional mice. Macroscopic findings were also confirmed on hematoxylin and eosin (H+E) staining, demonstrating large lung tumor deposits in control and only small or no microscopic lesions in XL184 groups. A significant difference in average lung weight was found between control (0.46 ± 0.11 g) and treated mice (0.23 ± 0.04 g; $P = 0.002$). Taken together, these results suggest that XL184 inhibits the growth of MPNST lung metastases.

Discussion

Knowledge of the molecular mechanisms driving MPNST development and progression is currently fragmentary. The loss of neurofibromin, the protein product of the *NF1* gene, is the molecular hallmark of NF1 and is suggested to be the primary tumor initiating event; NF1 loss has also been documented in sporadic MPNST (37, 38). However, additional genetic and epigenetic deregulations are required for malignant progression and acquisition of a metastatic phenotype. Alterations in major tumor-associated nodes/pathways such as p53, RB1, p16, p14, and p27 have been identified to occur exclusively in MPNSTs as compared with their benign neurofibroma counterparts (39, 40). Establishing MPNST-associated molecular aberrations amenable to therapeutic manipulation is a major investigational priority. To achieve that end, and justified by previously published data (14, 22, 24), the current study focused on the potential role of the MET-signaling pathway in MPNST. MET and its ligand HGF were found to be highly expressed in a relatively large panel of human MPNST samples. Furthermore, increased pMET expression levels were found to directly correlate with shorter MPNST patient survival. These observations are of potential major clinical relevance as sensitive MPNST-related molecular prognosticators could offer a heretofore lacking valuable tool to positively impact on patient surveillance and management. MET expression and activation have been associated with prognosis in a number of other tumor types (41, 42) and, most importantly, have been found to predict response to MET inhibitors (43).

Aberrant MET signaling in cancer has demonstrably broad protumorigenic, prometastatic functional effects (10). Among diverse effects, enhanced tumor cell proliferation and survival has been shown to commonly occur, possibly as a result of ERK and AKT pathways activation (11). Concordantly, HGF has previously been shown to be a Schwann cell (the proposed MPNST cell of origin) mitogen, significantly enhancing the proliferation of these cells (22). Interestingly, our investigations, consistent with a previously published study (24), failed to show a mitogenic, proproliferative effect of HGF/MET signaling in MPNST. In contrast, a significant impact on the migratory, invasive, and angiogenic phenotype of MPNST cells was observed *in vitro* and *in vivo*. These latter tumor-associated properties are essential for local aggressiveness and metastasis (10). The impact of HGF/MET on migration and invasion has previously been described and various molecular mechanisms underlying these capacities have been proposed. Our studies have identified HGF-induced MMP2 expression in MPNST cells as a possible mechanism for the observed enhanced tumor cell invasion. HGF is a known independent angiogenic factor mediating endothelial cell proliferation, survival, and motility through direct activation of MET expressed on these cells as well as through cooperation with VEGFR2 (44). Our data support an indirect proangiogenic effect of HGF/MET through the regulation of angiogenic factor expression by MPNST cells and tumor:endothelial cell cross-talk. Similarly, HGF-induced increases in the production of angiogenic cytokines IL-8 and VEGF by head and neck squamous cell carcinoma cell lines has previously been described (18). Taken together, our findings show a role for the HGF/MET autocrine loop in MPNST progression and metastatic spread.

Increasing knowledge of cancer-related deregulations undergirds the intensive efforts to develop drugs that eliminate tumor cells while sparing normal tissues. This target-orientated approach is aimed specifically at molecules that are involved in and contributing to cancer initiation and progression and are also easily "drugable." However, the vast majority of cancers defy single-molecule–directed therapy (45). Even malignancies which initially respond to such treatments usually develop resistance, and the tumors that emerge are often more aggressive and difficult to treat (45). These disappointing outcomes most probably reflect the extraordinary heterogeneity and complexity of cancer, involving numerous

Published OnlineFirst May 3, 2011; DOI: 10.1158/1078-0432.CCR-11-0193

molecular deregulations, genetic instability, and aneuploidy. In light of this complex reality, new agents or therapeutic combinations with broader specificity are being pursued in the hope that they will disable multiple nodes of vulnerability and simultaneously inhibit different procancer mechanisms. Our current study highlights the potential utility of MET as a potential MPNST therapeutic target potentially relevant to preventing or at least decreasing tumor recurrence and/or metastatic spread. As per the contemporary paradigm described above, we have elected to evaluate the preclinical effect of a novel compound, XL184, an ATP competitive and orally active inhibitor known to target MET and also other TKRs, specifically the angiogenic receptor VEGFR2 and the RET, KIT, FLT3, TIE2, and AXL receptors (35). Analogous to other solid malignancies, MPNSTs consist of both tumor cells and tumor-associated normal cells; the latter are potentially more susceptible to therapeutic targeting because of their relative genetic stability. MPNSTs are generally highly vascular and angiogenic; tumor:endothelial cell cross-talk results in increased metastatic potential (46). As reflected in our studies, targeting both tumor cells and tumor-associated endothelial cells using XL184 induces significant decrease in local and metastatic MPNST growth *in vivo*. XL184 has previously shown significant anticancer effects in preclinical models of brain, breast, lung, pancreatic, and thyroid cancers (35). Furthermore, the drug has been shown to reverse epidermal growth factor receptor (EGFR) inhibition resistance in lung cancer cells (47). An initial phase I clinical trial in patients with advanced solid malignancies showed XL184 to be well tolerated; generally only low-to-moderate severity side effects have been identified. Several phase I to III clinical trials for patients with medullary thyroid cancer, glioblastoma multiforme, and non–small cell lung carcinoma (NSCLC) are currently ongoing (47–49). Our results support the potential inclusion of patients with locally advanced and metastatic MPNST in such clinical investigations, especially given the dearth of other meaningful therapeutic interventions on behalf of this lethally challenged patient population. Development of novel XL184-containing therapeutic combinations should also be possibly considered.

Disclosure of Potential Conflicts of Interest

No potential conflicts of interest were disclosed.

Acknowledgments

The authors thank Dr. Thomas Mueller (Exelixis) for kindly providing XL184. The authors appreciate the expert assistance provided by Mr. Paul Cuevas in the preparation and submission of this manuscript, and Ms. Kim Vu for her aid in figure preparation. Anti-MET lentiviral shRNA constructs were developed and provided by the Cancer Biology Core Facility.

Grant Support

This manuscript was supported in part by a RTOG seed grant (to D. Lev), a National Foundation for Cancer Research (NFCR) – Hope Fund Seed Grant (to D. Lev), and an Amschwand Foundation Seed Grant (to D. Lev). D. Lev is supported by a NIH/NCI RO1CA138345, K. Torres by a 5T32CA009599–21 training grant, and M. Ghadimi by a Deutsche Forschungs Gemeinschaft training grant. The MDACC cell line characterization Core Facility was further supported by an NCI Cancer Center Support Grant (CA#16672).

The costs of publication of this article were defrayed in part by the payment of page charges. This article must therefore be hereby marked *advertisement* in accordance with 18 U.S.C. Section 1734 solely to indicate this fact.

Received January 22, 2011; revised April 5, 2011; accepted April 21, 2011; published OnlineFirst May 3, 2011.

References

1. Anghileri M, Miceli R, Fiore M, Mariani L, Ferrari A, Mussi C, et al. Malignant peripheral nerve sheath tumors: prognostic factors and survival in a series of patients treated at a single institution. Cancer 2006;107:1065–74.
2. Evans DG, Baser ME, McGaughran J, Sharif S, Howard E, Moran A. Malignant peripheral nerve sheath tumours in neurofibromatosis 1. J Med Genet 2002;39:311–4.
3. Zou C, Smith KD, Liu J, Lahat G, Myers S, Wang WL, et al. Clinical, pathological, and molecular variables predictive of malignant peripheral nerve sheath tumor outcome. Ann Surg 2009;249:1014–22.
4. Ducatman BS, Scheithauer BW, Piepgras DG, Reiman HM, Ilstrup DM. Malignant peripheral nerve sheath tumors. A clinicopathologic study of 120 cases. Cancer 1986;57:2006–21.
5. Wong WW, Hirose T, Scheithauer BW, Schild SE, Gunderson LL. Malignant peripheral nerve sheath tumor: analysis of treatment outcome. Int J Radiat Oncol Biol Phys 1998;42:351–60.
6. Traxler P, Bold G, Buchdunger E, Caravatti G, Furet P, Manley P, et al. Tyrosine kinase inhibitors: from rational design to clinical trials. Med Res Rev 2001;21:499–512.
7. Hueman MT, Schulick RD. Management of gastrointestinal stromal tumors. Surg Clin North Am 2008;88:599–614.
8. Rosen LS, Ashurst HL, Chap L. Targeting signal transduction pathways in metastatic breast cancer: a comprehensive review. Oncologist 2010;15:216–35.
9. Chao J, Chow WA, Somlo G. Novel targeted therapies in the treatment of soft-tissue sarcomas. Expert Rev Anticancer Ther 2010;10:1303–11.
10. Birchmeier C, Birchmeier W, Gherardi E, Vande Woude GF. Met, metastasis, motility and more. Nat Rev Mol Cell Biol 2003;4:915–25.
11. Maulik G, Shrikhande A, Kijima T, Ma PC, Morrison PT, Salgia R. Role of the hepatocyte growth factor receptor, c-Met, in oncogenesis and potential for therapeutic inhibition. Cytokine Growth Factor Rev 2002;13:41–59.
12. Cortner J, Vande Woude GF, Rong S. The Met-HGF/SF autocrine signaling mechanism is involved in sarcomagenesis. EXS 1995;74:89–121.
13. Fukuda T, Ichimura E, Shinozaki T, Sano T, Kashiwabara K, Oyama T, et al. Coexpression of HGF and c-Met/HGF receptor in human bone and soft tissue tumors. Pathol Int 1998;48:757–62.
14. Rao UN, Sonmez-Alpan E, Michalopoulos GK. Hepatocyte growth factor and c-MET in benign and malignant peripheral nerve sheath tumors. Hum Pathol 1997;28:1066–70.
15. Jeffers M, Schmidt L, Nakaigawa N, Webb CP, Weirich G, Kishida T, et al. Activating mutations for the met tyrosine kinase receptor in human cancer. Proc Natl Acad Sci U S A 1997;94:11445–50.
16. Ma PC, Jagadeeswaran R, Jagadeesh S, Tretiakova MS, Nallasura V, Fox EA, et al. Functional expression and mutations of c-Met and its therapeutic inhibition with SU11274 and small interfering RNA in non-small cell lung cancer. Cancer Res 2005;65:1479–88.
17. Ma PC, Tretiakova MS, MacKinnon AC, Ramnath N, Johnson C, Dietrich S, et al. Expression and mutational analysis of MET in human solid cancers. Genes Chromosomes Cancer 2008;47:1025–37.

Published OnlineFirst May 3, 2011; DOI: 10.1158/1078-0432.CCR-11-0193

18. Dong G, Chen Z, Li ZY, Yeh NT, Bancroft CC, Van Waes C. Hepatocyte growth factor/scatter factor-induced activation of MEK and PI3K signal pathways contributes to expression of proangiogenic cytokines interleukin-8 and vascular endothelial growth factor in head and neck squamous cell carcinoma. Cancer Res 2001;61:5911–8.
19. Liu X, Newton RC, Scherle PA. Developing c-MET pathway inhibitors for cancer therapy: progress and challenges. Trends Mol Med 2010;16:37–45.
20. Liu X, Yao W, Newton RC, Scherle PA. Targeting the c-MET signaling pathway for cancer therapy. Expert Opin Investig Drugs 2008;17:997–1011.
21. Peruzzi B, Bottaro DP. Targeting the c-Met signaling pathway in cancer. Clin Cancer Res 2006;12:3657–60.
22. Krasnoselsky A, Massay MJ, DeFrances MC, Michalopoulos G, Zarnegar R, Ratner N. Hepatocyte growth factor is a mitogen for Schwann cells and is present in neurofibromas. J Neurosci 1994;14:7284–90.
23. Mantripragada KK, Spurlock G, Kluwe L, Chuzhanova N, Ferner RE, Frayling IM, et al. High-resolution DNA copy number profiling of malignant peripheral nerve sheath tumors using targeted microarray-based comparative genomic hybridization. Clin Cancer Res 2008;14:1015–24.
24. Su W, Gutmann DH, Perry A, Abounader R, Laterra J, Sherman LS. CD44-independent hepatocyte growth factor/c-Met autocrine loop promotes malignant peripheral nerve sheath tumor cell invasion in vitro. Glia 2004;45:297–306.
25. Miller SJ, Rangwala F, Williams J, Ackerman P, Kong S, Jegga AG, et al. Large-scale molecular comparison of human Schwann cells to malignant peripheral nerve sheath tumor cell lines and tissues. Cancer Res 2006;66:2584–91.
26. Zou CY, Smith KD, Zhu QS, Liu J, McCutcheon IE, Slopis JM, et al. Dual targeting of AKT and mammalian target of rapamycin: A potential therapeutic approach for malignant peripheral nerve sheath tumor. Mol Cancer Ther 2009;8:1157–68.
27. Lahat G, Lazar A, Wang X, Wang WL, Zhu QS, Hunt KK, et al. Increased vascular endothelial growth factor-C expression is insufficient to induce lymphatic metastasis in human soft-tissue sarcomas. Clin Cancer Res 2009;15:2637–46.
28. Wang S, Ren W, Liu J, Lahat G, Torres K, Lopez G, et al. TRAIL and doxorubicin combination induces proapoptotic and antiangiogenic effects in soft tissue sarcoma *in vivo*. Clin Cancer Res 2010;16:2591–604.
29. McCarty MF, Baker CH, Bucana CD, Fidler IJ. Quantitative and qualitative *in vivo* angiogenesis assay. Int J Oncol 2002;21:5–10.
30. Lopez G, Liu J, Ren W, Wei W, Wang S, Lahat G, et al. Combining PCI-24781, a novel histone deacetylase inhibitor, with chemotherapy for the treatment of soft tissue sarcoma. Clin Cancer Res 2009;15:3472–83.
31. Torres K, Liu J, Young E, Huang F, Ghadimi M, Lusby K, et al. Expression of "drugable" tyrosine kinase receptors in MPNST: potential molecular therapeutic targets for a chemoresistant cancer. Histopathology. In press 2011.
32. Naldini L, Tamagnone L, Vigna E, Sachs M, Hartmann G, Birchmeier W, et al. Extracellular proteolytic cleavage by urokinase is required for activation of hepatocyte growth factor/scatter factor. EMBO J 1992;11:4825–33.
33. Di Renzo MF, Olivero M, Martone T, Maffe A, Maggiora P, Stefani AD, et al. Somatic mutations of the MET oncogene are selected during metastatic spread of human HNSC carcinomas. Oncogene 2000;19:1547–55.
34. Wasenius VM, Hemmer S, Karjalainen-Lindsberg ML, Nupponen NN, Franssila K, Joensuu H. MET receptor tyrosine kinase sequence alterations in differentiated thyroid carcinoma. Am J Surg Pathol 2005;29:544–9.
35. Zhang Y, Guessous F, Kofman A, Schiff D, Abounader R. XL-184, a MET, VEGFR-2 and RET kinase inhibitor for the treatment of thyroid cancer, glioblastoma multiforme and NSCLC. IDrugs 2010;13:112–21.
36. Joly A. Simultaneous blockade of VEGF and HGF receptors results in potent anti-angiogenic. EORTC Annual Meeting ; 2011; Brussels, Belgium; Abstract 104.
37. Basu TN, Gutmann DH, Fletcher JA, Glover TW, Collins FS, Downward J. Aberrant regulation of ras proteins in malignant tumour cells from type 1 neurofibromatosis patients. Nature 1992;356:713–5.
38. Bottillo I, Ahlquist T, Brekke H, Danielsen SA, Van Den Berg E, Mertens F, et al. Germline and somatic NF1 mutations in sporadic and NF1-associated malignant peripheral nerve sheath tumours. J Pathol 2009;217:693–701.
39. Mawrin C, Kirches E, Boltze C, Dietzmann K, Roessner A, Schneider-Stock R. Immunohistochemical and molecular analysis of p53, RB, and PTEN in malignant peripheral nerve sheath tumors. Virchows Arch 2002;440:610–5.
40. Zhou H, Coffin CM, Perkins SL, Tripp SR, Liew M, Viskochil DH. Malignant peripheral nerve sheath tumor: a comparison of grade, immunophenotype, and cell cycle/growth activation marker expression in sporadic and neurofibromatosis 1-related lesions. Am J Surg Pathol 2003;27:1337–45.
41. Kong DS, Song SY, Kim DH, Joo KM, Yoo JS, Koh JS, et al. Prognostic significance of c-Met expression in glioblastomas. Cancer 2009;115:140–8.
42. Oda Y, Sakamoto A, Saito T, Kinukawa N, Iwamoto Y, Tsuneyoshi M. Expression of hepatocyte growth factor (HGF)/scatter factor and its receptor c-MET correlates with poor prognosis in synovial sarcoma. Hum Pathol 2000;31:185–92.
43. Cepero V, Sierra JR, Corso S, Ghiso E, Casorzo L, Perera T, et al. MET and KRAS gene amplification mediates acquired resistance to MET tyrosine kinase inhibitors. Cancer Res 2010;70:7580–90.
44. Saucier C, Khoury H, Lai KM, Peschard P, Dankort D, Naujokas MA, et al. The Shc adaptor protein is critical for VEGF induction by Met/HGF and ErbB2 receptors and for early onset of tumor angiogenesis. Proc Natl Acad Sci U S A 2004;101:2345–50.
45. Hirsch FR, Mok TS, Borges V, Bunn PA Jr. Molecularly targeted therapy: when to stop and when to continue?Lancet Oncol 2010;11:709–11.
46. Kawachi Y, Xu X, Ichikawa E, Imakado S, Otsuka F. Expression of angiogenic factors in neurofibromas. Exp Dermatol 2003;12:412–7.
47. Wakelee HA, Gettinger SN, Engelman JA, Janne PA, West HJ, Subramaniam DS, et al. A phase Ib/II study of XL184 (BMS 907351) with and without erlotinib (E) in patients (pts) with non-small cell lung cancer (NSCLC). J Clin Oncol 2010;28suppl; abstr 3017.
48. Kurzrock R CE, Sherman SI, Pfister DG, Cohen RB, Ball D, et al. Long-term results in a cohort of medullary thyroid cancer (MTC) patients (pts) in a phase I study of XL184 (BMS 907351), an oral inhibitor of MET, VEGFR2, and RET. J Clin Oncol 2010;28suppl; abstr 5502.
49. Wen P, Prados M, Schiff D, Reardon D, Cloughesy T, Mikkelsen T, et al. Phase 2 study of XL184 (BMS-907351), an inhibitor of MET, VEGFR2, and RET in patients with progressive glioblastoma. J Clin Oncol 2010:28suppl; abstr 2006.